

RESEARCH ARTICLE

Characterization of whole-brain task-modulated functional connectivity in response to nociceptive pain: A multisensory comparison study

Linling Li^{1,2}  | Xin Di³ | Huijuan Zhang^{4,5} | Gan Huang^{1,2} | Li Zhang^{1,2}  | Zhen Liang^{1,2} | Zhiguo Zhang^{1,2,6}

¹School of Biomedical Engineering, Health Science Center, Shenzhen University, Shenzhen, China

²Guangdong Provincial Key Laboratory of Biomedical Measurements and Ultrasound Imaging, Shenzhen, China

³Department of Biomedical Engineering, New Jersey Institute of Technology, Newark, New Jersey, USA

⁴CAS Key Laboratory of Mental Health, Institute of Psychology, Chinese Academy of Sciences, Beijing, China

⁵Department of Psychology, University of Chinese Academy of Sciences, Beijing, China

⁶Peng Cheng Laboratory, Shenzhen, China

Correspondence

Zhiguo Zhang, No. 1066, Xueyuan Road, Nanshan District, Shenzhen, Guangdong, China.

Email: zgzhang@szu.edu.cn

Funding information

National Natural Science Foundation of China, Grant/Award Numbers: 81901831, 81871443; Natural Science Foundation of Guangdong Province, China, Grant/Award Number: 2021A1515011152; Shenzhen-Hong Kong Institute of Brain Science-Shenzhen Fundamental Research Institutions, Grant/Award Number: 2021SHIBS0003

Abstract

Previous functional magnetic resonance imaging (fMRI) studies have shown that brain responses to nociceptive pain, non-nociceptive somatosensory, visual, and auditory stimuli are extremely similar. Actually, perception of external sensory stimulation requires complex interactions among distributed cortical and subcortical brain regions. However, the interactions among these regions elicited by nociceptive pain remain unclear, which limits our understanding of mechanisms of pain from a brain network perspective. Task fMRI data were collected with a random sequence of intermixed stimuli of four sensory modalities in 80 healthy subjects. Whole-brain psychophysiological interaction analysis was performed to identify task-modulated functional connectivity (FC) patterns for each modality. Task-modulated FC strength and graph-theoretical-based network properties were compared among the four modalities. Lastly, we performed across-sensory-modality prediction analysis based on the whole-brain task-modulated FC patterns to confirm the specific relationship between brain patterns and sensory modalities. For each sensory modality, task-modulated FC patterns were distributed over widespread brain regions beyond those typically activated or deactivated during the stimulation. As compared with the other three sensory modalities, nociceptive stimulation exhibited significantly different patterns (more widespread and stronger FC within the cingulo-opercular network, between cingulo-opercular and sensorimotor networks, between cingulo-opercular and emotional networks, and between default mode and emotional networks) and global property (smaller modularity). Further, a cross-sensory-modality prediction analysis found that task-modulated FC patterns could predict sensory modality at the subject level successfully. Collectively, these results demonstrated that the whole-brain task-modulated FC is preferentially modulated by pain, thus providing new insights into the neural mechanisms of pain processing.

KEYWORDS

functional connectivity, MRI, neuroimaging, pain, psychophysiological interaction, task

This is an open access article under the terms of the Creative Commons Attribution-NonCommercial-NoDerivs License, which permits use and distribution in any medium, provided the original work is properly cited, the use is non-commercial and no modifications or adaptations are made.

© 2021 The Authors. *Human Brain Mapping* published by Wiley Periodicals LLC.

1 | INTRODUCTION

Pain perception activates multiple brain regions, such as the primary and secondary somatosensory cortices, insula, and anterior cingulate cortex, which are often termed as the “pain matrix” (Apkarian, Bushnell, Treede, & Zubieta, 2005). However, the “pain matrix” can also be activated by stimuli of other sensory modalities (Downar, Crawley, Mikulis, & Davis, 2000; Iannetti & Mouraux, 2010; Legrain, Iannetti, Plaghki, & Mouraux, 2011). For example, Mouraux, Diukova, Lee, Wise, and Iannetti (2011) compared functional magnetic resonance imaging (fMRI) responses to nociceptive pain and other three sensory modalities (non-nociceptive somatosensory, visual, auditory), and found that different sensory modalities elicited extremely similar responses in a wide distribution of brain areas, which mainly reflect multimodal brain processes crucial for all sensory systems. Recently, some fMRI studies used experimental manipulation to identify brain activities preferentially involved in pain perception. For example, Su et al. (2019) found that nociceptive and non-nociceptive somatosensory stimuli elicit activations in overlapping brain regions, but some of these regions, such as the opercular cortex and supplementary motor area, were more strongly engaged in the processing of nociceptive pain. On the other hand, because the brain is functionally integrated, external tasks could induce specific changes in widespread brain networks (Gonzalez-Castillo & Bandettini, 2018). However, the task-modulated functional connectivity (FC) patterns elicited by nociceptive pain and other sensory modalities remain unclear, which limits our investigation of brain activities preferentially involved in pain perception from a brain network perspective.

FC analysis was performed for acute pain and tonic pain experiments and it was found that FC between the posterior insula and the default mode network may differentiate painful state from nonpainful resting-state (Ibinson et al., 2015; Vogt, Becker, Wasan, & Ibinson, 2016). In these studies, FC patterns were characterized by regressing out of the mean task activation and the estimating of the correlation coefficients of the residuals (Cole et al., 2019). Therefore, this approach cannot be used to test the hypothesis that the FC pattern should vary depending on the experimental conditions in a single run, which is necessary for the investigation of FC changes related to stimulation of different sensory modalities (Cole et al., 2019). Another widely accepted task-modulated FC estimation approach is psychophysiological interaction (PPI), which measures whether and how FC between brain regions varies with different experimental conditions (Di, Zhang, & Biswal, 2020; O'Reilly, Woolrich, Behrens, Smith, & Johansen-Berg, 2012). PPI has been used to investigate top-down modulation of acute pain in healthy subjects (Ploner, Lee, Wiech, Bingel, & Tracey, 2011; Reicherts et al., 2017). For example, regarding the cognitive-affective domain of pain perception, a stronger PPI effect was observed between the amygdala of the emotional network and the anterior insula of the cingulo-opercular network (Reicherts et al., 2017). However, these earlier investigations of task-modulated FC in pain-related studies were limited to the activated region of interest (ROI), and FC involving brain regions that are not classically known to be part of the “pain matrix” are often overlooked (Kucyi &

Davis, 2015; Necka et al., 2019). But in fact, one recent study has used the whole-brain PPI analysis to reveal a much broader involvement of brain regions in task-modulated FC than those only including regional activations (Di & Biswal, 2019).

Perception of external sensory stimulation requires complex interactions among distributed cortical and subcortical brain regions. Such as the default mode network, which is perhaps the most studied large-scale brain network, and task-positive networks usually interact with the default mode network during perception of external sensory stimulation (Elton & Gao, 2015). As one of the task-positive networks, the cingulo-opercular network, also known as the “salience network,” is generally believed to undertake the fundamental function of tonic alertness by integrating sensory information (Sadaghiani & D'Esposito, 2015). According to previous studies, a number of brain structures within the cingulo-opercular network, such as the anterior insula/operculum, dorsal anterior cingulate cortex, and thalamus, are consistently activated during pain stimulation (Borsook, Edwards, Elman, Becerra, & Levine, 2013). Considering its closer relationship with pain perception, the cingulo-opercular network might show stronger within- and between-network task-modulated FC strength. Besides, the topological architecture (i.e., small-worldness) of resting-state brain networks is related to cognitive performance during the task (Bullmore & Bassett, 2011; Cohen & D'Esposito, 2016). Considering the high-level activities involved during pain perception, the reconfiguration of brain networks might be different compared with other sensory modalities.

Hence, in the present study, we used an experimental design of four sensory modalities (nociceptive somatosensory, non-nociceptive somatosensory, visual, and auditory) and whole-brain PPI analysis to characterize task-modulated FC patterns in response to the stimulation of different sensory modalities. Besides, we checked whether the task-modulated FC patterns were predictive of sensory modalities at the subject level, in order to show the extracted task-modulated FC patterns elicited by different sensory modalities were accurate and reliable. In this cross-sensory-modality prediction analysis, if task-modulated FC patterns are able to predict sensory modalities, it means these FC patterns contain important and inherent information that is preferentially or even specific to the type of incoming sensory stimulation. We expected all sensory modalities to induce widespread task-modulated FC within and between many brain networks. But we hypothesized that due to the specific aspects of pain perception, regional and global features of task-modulated FC in a number of brain networks, such as the default mode and cingulo-opercular networks, would show distinguishing differences for nociceptive pain compared with the other sensory modalities.

2 | MATERIALS AND METHODS

2.1 | Participants

A total of 80 healthy subjects (36 males/44 females, 21 ± 3 years) participated in this study. All subjects were free of acute or chronic

pain and gave their written informed consent. The experimental procedures were approved by the ethics committee of the Institute of Psychology, Chinese Academy of Sciences (date of approval: November 2016; approval number: H16021).

2.2 | Experimental paradigm

The experiment of task fMRI acquisition was divided into two sessions. Subjects received brief stimuli of four different sensory modalities: nociceptive somatosensory, non-nociceptive somatosensory, auditory, and visual. Nociceptive radiant heat somatosensory stimuli were generated by an infrared neodymium yttrium aluminum perovskite (Nd: YAP) laser and delivered on the dorsum of the subject's left hand (ulnar and radial nerve dermatome). The diameter of the laser beam was set at approximately 7 mm and the pulse duration was 50 ms. Non-nociceptive somatosensory stimuli (transcutaneous electrical stimuli) consisted of nonpainful constant-current square-wave pulses (1,000 Hz frequency, 1,000 ms pulse width, and 50 ms pulse duration) delivered through a pair of electrodes attached on the median nerve of the left forearm, separated by a 1 cm interelectrode distance. Diotic auditory stimuli consisted of brief 800 Hz pure tones (500 ms duration, 5 ms rise and fall times) were delivered through pneumatic tubing to earphones inserted inside the acoustic canals. Visual stimuli consisted of a gray disk displayed on the projection screen for 100 ms. Each type of stimuli included two intensity levels: 3 J and 3.5 J for nociceptive somatosensory stimuli, 2 mA and 4 mA for non-nociceptive somatosensory stimuli, 76 dB SPL and 88 dB SPL for auditory stimuli, two gray images with different gray scale values for visual stimuli. The two levels of intensities were determined for each sensory modality based on a preliminary psychophysical experiment performed on 10 healthy subjects (three males) recruited from the same cohort as the subjects included in the formal experiment. The physical intensities corresponding to the perceived intensity rating of 4 and 6 were used in the subsequent experiment as the low and high stimulus intensities, respectively. Within each run, each type of stimulation was delivered 10 times in a pseudo-random order, 5 times for each level. The inter-stimulus interval was randomized between 21 s and 24 s. There was an interval of 6 s between the onset of the trial and the onset of the stimulus period, and an interval of 10 s between the stimulation period and the beginning of the rating period. A white fixation cross was displayed at the center of the screen during the first 6 s period. The stimulation period was 50 ms for nociceptive and non-nociceptive somatosensory, 100 ms for visual, and 500 ms for auditory. During the 5 s of the rating period, a visual analogue scale (VAS, ranging from 0 to 10) was presented on the screen, and subjects were asked to rate the intensity of each stimulus using a button box (moving the cursor to the location of corresponding rating number). Stimulus intensity was explained to subjects as "how intense do you feel the stimulation of this sensory modality" and the lower and upper ends of the scale were defined as "no sensation of such modality" and "the most intense sensation tolerable" respectively. Taking the laser stimulation as an example,

0 means no feeling of pain, and 10 means the most intense pain intensity that can be tolerated.

2.3 | MRI data acquisition and preprocessing

fMRI data were collected using a GE 3.0 T MRI scanner. A standard gradient echo planar imaging sequence with the following imaging parameters was used: 43 oblique slices, thickness/gap = 3/0 mm, acquisition matrix = 64×64 , time of repetition = 2000 ms, time of echo = 30 ms, flip angle = 90° , field of view = $192 \times 192 \text{ mm}^2$. For the multi-sensory stimulation task, two sessions with 454 functional volumes were administered. A resting-state session with 300 volumes was also collected, with the aim to estimate baseline resting-state FC for comparison with task-modulated FC. In the resting-state session, subjects were asked to stay motionless, relax their minds and focus at a "+" fixation sign on the screen.

fMRI data preprocessing was performed using Statistical Parametric Mapping (SPM12, www.fil.ion.ucl.ac.uk/spm/software/spm12). Data preprocessing steps include: (1) the first three volumes of each functional time-series were removed for magnetization equilibrium; (2) for each participant, the images were corrected for differences in the intravolume acquisition time between slices using sinc interpolation and then corrected for intervolumetric geometric displacement due to head movement using a six-parameter (rigid-body) spatial transformation; (3) the anatomical T1 image was coregistered to the mean functional image, created during the former step; (4) functional images were spatially normalized to common template image (T1 template in Montreal Neurological Institute standard space) using the unified normalization-segmentation procedure via the structural T1 images and resampled to a voxel size of $3 \times 3 \times 3 \text{ mm}^3$; (5) spatial smoothing was performed using 6 mm full-width at half maximum (FWHM) Gaussian kernel.

2.4 | Parcellation atlas

Whole-brain parcellation was adopted using Dosenbach's 160 ROIs (Dosenbach et al., 2010). The identification of nodes (i.e., ROIs) is the key factor in studying the properties of FC, but anatomical atlas, such as the AAL atlas, contained little information about FC, and their capacity for accurately representing FC was limited (Craddock et al., 2013). The selected Dosenbach 160-region atlas was generated based on a meta-analysis of task-related fMRI data, and it is more reliable and suitable for the construction of FC networks than anatomical atlases (Yao, Hu, Xie, Moore, & Zheng, 2015). We excluded 20 cerebellar ROIs for incomplete coverage of the cerebellum of several subjects and included four extra ROIs related to emotional processing (Di, Gohel, Kim, & Biswal, 2013; Sabatinelli et al., 2011): the right amygdala (Montreal Neurological Institute, MNI, coordinates: 20, -4, -15), the left amygdala (-20, -6, -15), the right parahippocampus (14, -33, -7), and the left parahippocampus (-20, -33, -4). These selected 144 ROIs made up six FC networks according to Dosenbach

atlas: (1) cingulo-opercular network, (2) default mode network, (3) frontoparietal network, (4) occipital network, (5) sensorimotor network, and (6) emotional network (Dosenbach et al., 2010).

2.5 | Resting-state functional connectivity (FC) analysis

Resting-state FC was estimated to provide a reference or baseline for task-modulated FC. Additional postprocessing steps were performed on the preprocessed resting-state fMRI data. First, the following nuisance variables were regressed out from resting-state data: linear trend, 24 head motion regressors, mean signals of white matter, and cerebrospinal fluid. Then the data were then temporal band-pass filtered (0.01–0.1 Hz). The mean time series of all 144 ROI was extracted and the Pearson's correlations were calculated between all pairs of ROIs. The obtained correlation matrix for each subject was normalized using Fisher's z-transformation.

2.6 | GLM analysis of task fMRI data for activation detection

In order to extract ROI time series for ROI-based activation analysis and PPI analysis, voxel-wise general linear model (GLM) analysis was performed in MATLAB relying on the SPM12 toolbox and custom-made MATLAB scripts. Because this task was divided into two sessions for each subject, the data of these two sessions were modeled as separate regressors and covariates in a single subject-level GLM. Specifically, for each session, the occurrence of the stimuli from each modality was modeled as a separate regressor with parametric modulation by their corresponding VAS ratings, and the rating period was also modeled as an additional regressor. Head motion parameters (six rigid-body transformations, their one time-point lags, and all their correspondent squared time series), and the mean of each session was included as covariates in the GLM. After model estimation, an "effects of interest" F-contrast was defined. For each of the 144 ROIs, the first Eigen variate (principal component) of the time courses within this ROI was extracted for each run. Effects of no interest (24 head motion regressors, including 6 rigid-body transformations, their one time-point lag, and all their correspondent squared time series) were adjusted to minimize the head motion effects. Note that, the time series of ROIs used in the GLM for PPI analyses were the same as those in the GLM analyses for ROI-wised activations.

ROI-wise activation analysis was also performed to compare the regional activation results with later PPI results. Similar GLMs as in the voxel-wise analysis but without nuisance regressors were applied to the ROI time series because the effects of no-interest have been removed during the time series extraction. After model estimation, four contrasts of interests were calculated, corresponding to the activation by the stimulation of four sensory modalities of each subject. The contrast maps for each sensory modality were used in further group analysis.

2.7 | Psychophysiological interaction analysis

In the present study, task-modulated FC was inferred from PPI effects using the generalized PPI framework, which models each task condition separately with reference to all other conditions and then compare the PPI effects between the conditions of interests (McLaren, Ries, Xu, & Johnson, 2012). The time-series of an ROI was first deconvolved with the hemodynamic response function (HRF), and then point-by-point multiplied with the psychological variable of each sensory modality to form the PPI term of neuronal level (Di, Reynolds, & Biswal, 2017). Next, the PPI terms of neuronal level were convolved with the HRF to obtain the blood-oxygen-level-dependent level PPI terms. Then single subject-level GLM for PPI effect analysis was built with 10 explanatory variables (four regressors of task conditions for each sensory modality, four regressors of PPIs calculated for each sensory modality, the time series of the ROI, and one constant term) for each ROI, and were fitted to the time-series of all other ROIs (as dependent variable) separately. Because a constant term that represents the overall effect (intercept) is usually added in a regression model, when modeling n conditions, we need $n-1$ additional regressors. In present study, we utilized an event-related design, and all the experimental conditions were included, and the baseline condition was left out of the model (implicit baseline). Therefore, regressors of PPI terms in this GLM model represented the differences between the modeled stimulation conditions with respect to all the other conditions (Di et al., 2020). After estimation of GLM, the contrasts of interest were the PPI effect for each sensory modality. This process was repeated for every ROI pair (i.e., for a given target ROI, the modeling was repeated for every other ROI as the predictor ROI), yielding a 144×144 asymmetric contrast matrix for each sensory modality and each subject. PPI approach measures the task-modulated FC changes in terms of the strength of regression of activity in one region on another; however, it does not make an inference about the direction of information flow (Friston et al., 1997; McLaren et al., 2012). Therefore, the PPI matrix was symmetrized by averaging them with their transpose (Di et al., 2017). The symmetric PPI matrices for all four sensory modalities were used in further group analysis.

2.8 | Calculation of graph-theoretical network metrics of task-modulated FC

Graph-based network analysis reveals meaningful information about the topological architecture of human brain networks. Task-fMRI-based brain networks can be constructed with ROIs as nodes and task-modulated FC strength (PPI effects) as edges. In addition to localizing specific FC modulated by a sensory modality, a further question is the topological reconfiguration of the brain in response to external stimulation of different sensory modalities. To characterize different characteristics of network reconfiguration during stimulation of four sensory modalities, global network metrics were calculated by using the Brain Connectivity Toolbox (brain-connectivity-toolbox.net) (Rubinov & Sporns, 2010). First, binary unidirectional networks were

built for each sensory modality and each subject by thresholding the absolute task-modulated FC matrix at 10, 20, and 30% sparsity levels respectively. Enforcing the same sparsity levels among the four sensory modalities could ensure that the differences observed in the network properties are not due to the difference in the number of edges. These sparsity levels were used because the large-scale brain networks revealed small-world properties within the range of 6–40% (Achard & Bullmore, 2007). We calculated two representative small-world metrics, the global efficiency and mean clustering coefficient, and the modularity for these thresholded task-modulated FC networks (Bullmore & Sporns, 2009). The global efficiency characterizes the efficiency of information integration of the whole network, and the mean clustering coefficient characterizes the efficiency of the information flow around local nodes in a network (Watts & Strogatz, 1998). The modularity characterizes the extent to which the network can be divided into sub-communities (Newman, 2006).

2.9 | Cross-sensory-modality prediction based on task-modulated FC

Lastly, we checked whether the task-modulated FC patterns were predictive of sensory modalities at the subject level. Specifically, we performed across-sensory-modality prediction analysis based on the whole-brain task-modulated FC features. First, a template was computed for each sensory modality by averaging the task-modulated FC matrices of ($N-1$) subjects, where N is the total number of subjects. The task-modulated FC matrices of the remaining one subject were used as the target matrices. To predict the sensory modality, the similarity between the target matrix and the template matrix of each sensory modality was computed as the Pearson correlation coefficient between the vectorized target matrix and template matrix, and the predicted sensory modality was the one with the maximal similarity score. This procedure was repeated for N times so that prediction accuracy for each sensory modality was calculated.

2.10 | Statistical analysis

All statistical analyses were performed using the MATLAB (MathWorks Inc., MA) or SPSS (SPSS Statistics, IBM, Armonk, NY) software.

2.10.1 | Behavioral data analysis

For each subject and each sensory modality, the mean VAS rating of all stimuli was calculated. Further, we adopted one-way repeated-measure ANOVA (factor: sensory modality) to investigate differences in subjective ratings across sensory modalities. We compared the ratings of different stimuli because we wanted to make sure that the

differences of FC were not caused by differences in perceived stimulus intensity. Otherwise, FC differences of different sensory modalities may be caused by the differences in ratings. In another word, “ratings” could be a confounding factor when comparing FC of different sensory modalities, so ratings should be well controlled (i.e., to make it comparable across different sensory modalities).

2.10.2 | Group-level analysis of resting-state FC

For group-level analysis of resting-state FC, the one-sample t -tests were performed on Fisher r -to- z -transformed correlation matrices and false discovery rate (FDR) correction was used for multiple comparisons (Benjamini & Hochberg, 1995; Benjamini & Yekutieli, 2001).

2.10.3 | Group-level analysis of ROI-wise GLM activations

In order to examine the average activation during each condition, contrast maps extracted from subject-level ROI-wise GLM analyses were entered into a second-level one-sample t -test to obtain group-level results after FDR correction.

2.10.4 | Group-level analysis of task-modulated FC strength

Group-level analysis of task-modulated FC was performed to compare within- and between-network FC strength (PPI effects) between conditions of interest. For each sensory modality, one-sample t -test across subjects was performed for group effect of each condition at each pair of ROIs with FDR correction. After the group analysis, all the ROI pairs with significant group main effect were extracted for each sensory modality. These ROI pairs were grouped according to the selected brain parcellation atlas (within and between these networks) and mean FC strength was calculated for each sensory modality. Then one-way repeated-measure ANOVA was performed to assess the difference of within- and between-network FC strength among the four sensory modalities. FDR correction was applied for multiple comparisons. For within- or between-network FC which showed significant differences among four modalities, pairwise comparisons were performed using Bonferroni post hoc tests.

2.10.5 | Group-level analysis of network metrics of task-modulated FC

To investigate different characteristics of network reconfiguration during stimulation of four sensory modalities, one-way repeated-measure ANOVA and Bonferroni post hoc tests were performed to make a comparison of network metrics.

2.10.6 | Permutation tests for cross-sensory-modality prediction performance

To assess the statistical significance of the prediction accuracy for each sensory modality, we performed nonparametric permutation testing of 1,000 repetition times. In each iteration, the class labels of the template matrices were randomly permuted. The real prediction accuracy was then compared with the randomized distribution to determine statistical significance.

3 | RESULTS

3.1 | Subjective ratings

Average VAS ratings for four sensory modalities are: 4.9 ± 1.5 for nociceptive somatosensory stimulation, 4.7 ± 1.3 for non-nociceptive somatosensory stimulation, 4.8 ± 1.1 for visual stimulation, and 4.6 ± 1.2 for auditory stimulation. One-way repeated-measures ANOVA of VAS ratings showed no significant difference among the four sensory modalities ($p = .124$; as shown in Figure 1).

3.2 | GLM activations

According to ROI-wise GLM analysis results (as shown in Figure 2 and Table S1), stimulation of different sensory modalities elicited activations in widely distributed and largely overlapping brain regions, including the primary sensory cortices (such as the postcentral gyrus for somatosensory perception, the superior temporal cortex for auditory perception, and the occipital cortex for visual perception), and brain areas related to higher cognitive functions (such as the cingulo-opercular and fronto-parietal regions). On the other hand, deactivation was mainly observed in brain areas belonging to the default mode

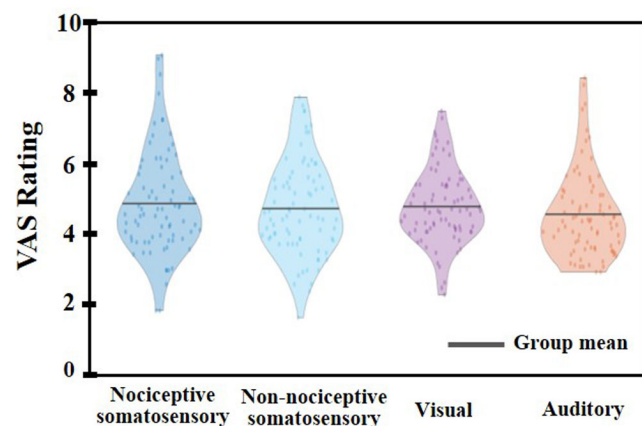


FIGURE 1 Visual analogue scale (VAS) ratings of four modalities of stimulation: nociceptive somatosensory, non-nociceptive somatosensory, visual, and auditory. Each dot denotes the averaged VAS rating of one participant

network (such as the medial prefrontal cortex), the left precentral gyrus, and the occipital cortex.

3.3 | PPI analysis results

3.3.1 | Resting-state FC and task-modulated FC

Figure 3 illustrates the raw and FDR-corrected matrices of resting-state FC and task-modulated FC of four sensory modalities. During resting-state, significant within-network FC was observed for all six networks, and the default mode network is anticorrelated with other networks, such as the cingulo-opercular and sensorimotor networks (Figure 3, left panel). As shown in the right panel of Figure 3, the PPI analysis revealed that four sensory modalities all elicited statistically significant task-modulated FC. During the stimulation of each sensory modality, both positive and negative FC were observed, and they all covered many different brain networks. Different from the resting-state FC, within-network FC turned negative during tasks. For all four sensory modalities, positive FC was mainly observed between the default mode network and other networks, including the frontal-parietal, occipital and sensorimotor networks, while negative FC was observed between the occipital and emotional networks.

Most previous PPI studies only focused on the brain regions which showed task-related regional activations. In this study, intermixed positive/negative task-modulated FC was observed not only among activated brain regions but also among deactivated and even nonactivated brain regions for all sensory modalities (as shown in Figure S1). For increased FC of each sensory modality, there was a clear-cut pattern showing that one node is a task-activated brain region, and the other one can be activated, deactivated, or not activated. For example, nociceptive somatosensory stimulation elicited significant activation over brain regions of the cingulo-opercular network (e.g., the anterior cingulate cortex and anterior insula). We can find increased connectivity between these activated regions and other activated regions (e.g., the precuneus and post cingulate cortex of the default mode network), deactivated regions (e.g., the ventral medial prefrontal cortex of the default mode network), and nonactivated regions (e.g., the anterior prefrontal cortex and inferior parietal cortex of the fronto-parietal network).

3.3.2 | Comparison of task-modulated FC strength across sensory modalities

To better illustrate the difference of task-modulated FC among four sensory modalities, we compared the mean FC strengths (PPI effects) using one-way repeated-measure ANOVA (see Figure 4). FC strengths were calculated as the contrasts of interest (arbitrary units) using the constructed GLM models for PPI analysis. Compared with the other three sensory modalities, the nociceptive somatosensory stimulation elicited relatively stronger positive FC between the cingulo-opercular and sensorimotor networks, between the cingulo-opercular and

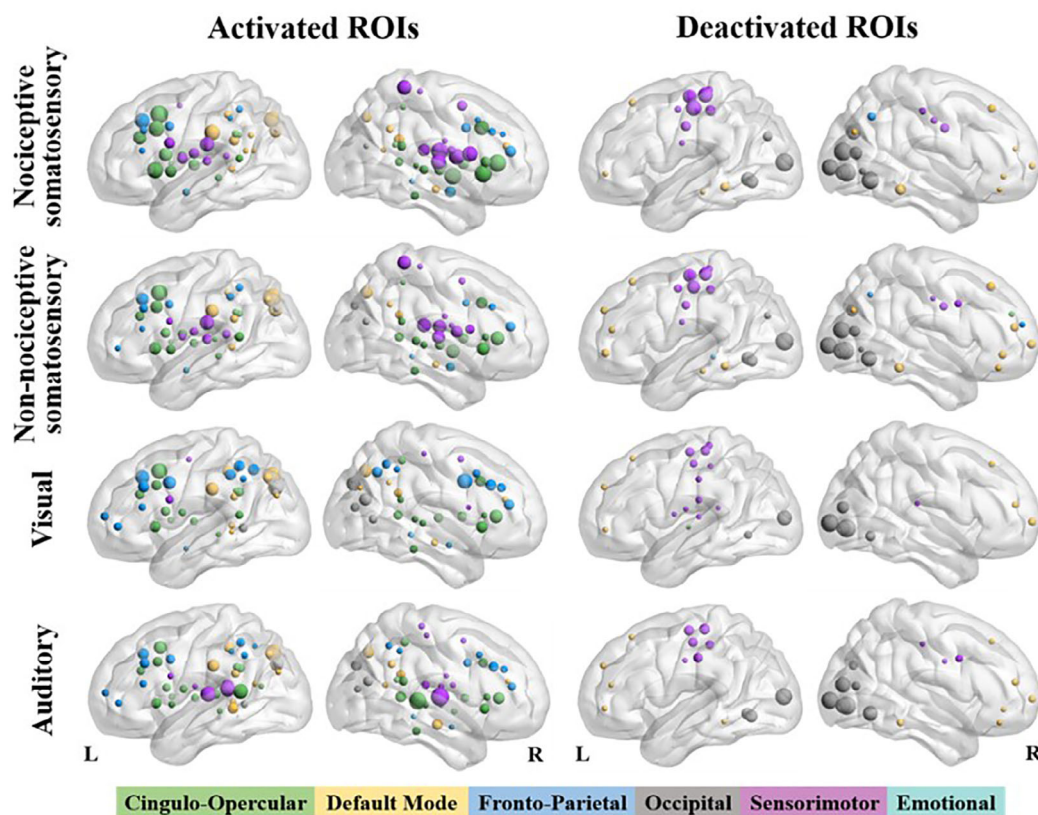


FIGURE 2 Region of interest (ROI)-wise general linear model (GLM) analysis results. Activated and deactivated ROIs during nociceptive, non-nociceptive, visual, and auditory stimulation. Significant results were identified at $p < .05$ with FDR correction. The size of each node (ROI) is in proportion to the mean contrast values of the ROI

emotional networks, between the default mode and emotional networks, and between the sensorimotor and emotional networks. Differently, non-nociceptive somatosensory stimulation elicited significantly stronger negative FC within the cingulo-opercular and default mode networks, between the cingulo-opercular and emotional networks, and between the default mode and emotional networks. During the visual stimulation, significant FC was observed between the cingulo-opercular and occipital networks, between the sensorimotor and occipital networks, and within the fronto-parietal network. For the auditory stimulation, we also observed positive connections between the cingulo-opercular and occipital networks, between the cingulo-opercular and sensorimotor networks, but the FC strength was relatively weaker than the other three sensory modalities. It should be noted that no ROI pair within the emotional network was obtained for significant group effect during nociceptive somatosensory and visual stimulation, so the mean FC strength within the emotional network was not compared among the four sensory modalities.

3.3.3 | Comparison of graph-theoretical network metrics of task-modulated FC

For comparison of graph-theoretical network metrics of task-modulated FC networks, binary unidirectional networks were built by

thresholding the absolute task-modulated FC matrix at 10%, 20%, and 30% sparsity levels, respectively. Using the same sparsity levels could ensure that the differences observed in the network metrics are not due to the difference in the number of edges. According to the results, one-way repeated-measures ANOVA revealed a significant effect of sensory modality for modularity at sparsity levels of 10% ($F = 5.440$, $p = .001$) and 20% ($F = 3.759$, $p = .012$). Furthermore, significant post hoc pair-wise differences of modularity were observed between nociceptive somatosensory and visual, between nociceptive somatosensory and auditory, and between non-nociceptive somatosensory and auditory (Figure 5a). However, no significant difference was observed for the other two network metrics: the global efficiency and clustering coefficient (Figure 5b,C).

3.3.4 | Cross-sensory-modality prediction based on task-modulated FC

Table 1 shows the performance of using the whole-brain task-modulated FC matrices as features to predict sensory modality. The successful rate was 44% ($p < .001$) for nociceptive somatosensory, 25% ($p = .428$) for non-nociceptive somatosensory, 38% ($p = .003$) for visual, and 40% ($p = .001$) for auditory. Except for non-nociceptive somatosensory, all other three sensory modalities had

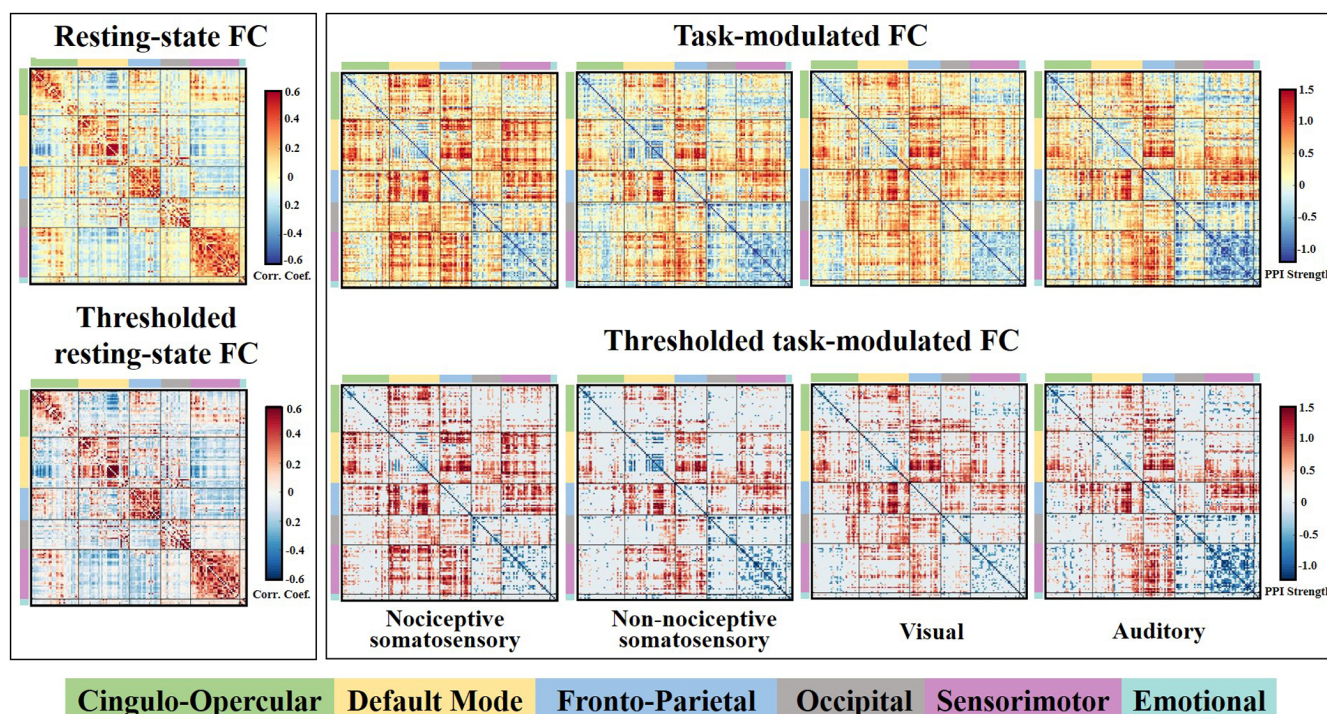


FIGURE 3 Left panel: whole-brain resting-state functional connectivity (FC) matrices, unthresholded (top row) and thresholded (bottom row; $p < .05$, FDR corrected). Right panel: whole-brain task-modulated FC matrices for nociceptive somatosensory, non-nociceptive somatosensory, visual, and auditory, unthresholded (top row) and thresholded (bottom row; $p < .05$, FDR corrected). The color bars on the left and on the top side of each matrix represent 6 functional brain networks: (1) cingulo-opercular, (2) default mode, (3) fronto-parietal, (4) occipital, (5) sensorimotor, and (6) emotional networks

prediction accuracies significantly greater than the chance level (25%).

4 | DISCUSSION

In this study, we hypothesized that regional and global features of task-modulated FC in a number of brain networks, such as the default mode and cingulo-opercular networks, would show distinguishing differences for nociceptive pain compared with other sensory modalities. To validate this hypothesis, we characterized the differences in task-modulated FC (as measured by PPI) elicited by stimuli of four sensory modalities (nociceptive somatosensory, non-nociceptive somatosensory, visual, and auditory), which were delivered in random order. Our results indicate positive/negative task-modulated FC was distributed over widespread areas for all four sensory modalities, and task-modulated FC of nociceptive somatosensory showed significantly different regional and global task-modulated FC features from those of the other three sensory modalities.

4.1 | Task-modulated local activity and FC

Neuroimaging studies of pain revealed distributed brain regions of regional activations (Duerden & Albanese, 2013), and found that

different sensory modalities elicited extremely similar responses, which mainly reflect multimodal brain processes crucial for all sensory systems (Mouraux et al., 2011). In accordance with that, GLM activation analysis here also revealed that stimuli of pain and other three sensory modalities elicited very similar brain responses all over the six brain networks (Mouraux et al., 2011). Specifically, similar to nociceptive somatosensory stimuli, the application of the other three types of sensory modalities also produces significant activations within the “pain matrix,” such as the thalamus, insula, cingulate cortex. Besides, deactivations were observed in regions of the default mode network, such as the medial prefrontal cortex, as well as in the lateral occipital regions, contralateral somatosensory areas, and premotor area. Previous studies suggested the functional dissociation between activated and deactivated brain regions, and the deactivations were normally interpreted in terms of shifting attention, cross-modal inhibition, and withdrawal of unnecessary movement (Kong et al., 2010). An in-depth investigation of GLM-based activation/deactivation is definitely useful and interesting, but it is beyond the scope of this work (focusing on task-modulated FC). Future experiments and analyses will be needed to clarify the functional dissociation between task-modulated FC patterns of activated and deactivated regions.

Previously published multisensory studies were mainly focused on the comparison of regional activations (Iannetti & Mouraux, 2010; Legrain et al., 2011; Liang, Mouraux, Hu, & Iannetti, 2013; Liang, Su, Mouraux, & Iannetti, 2019), but only investigating local activation

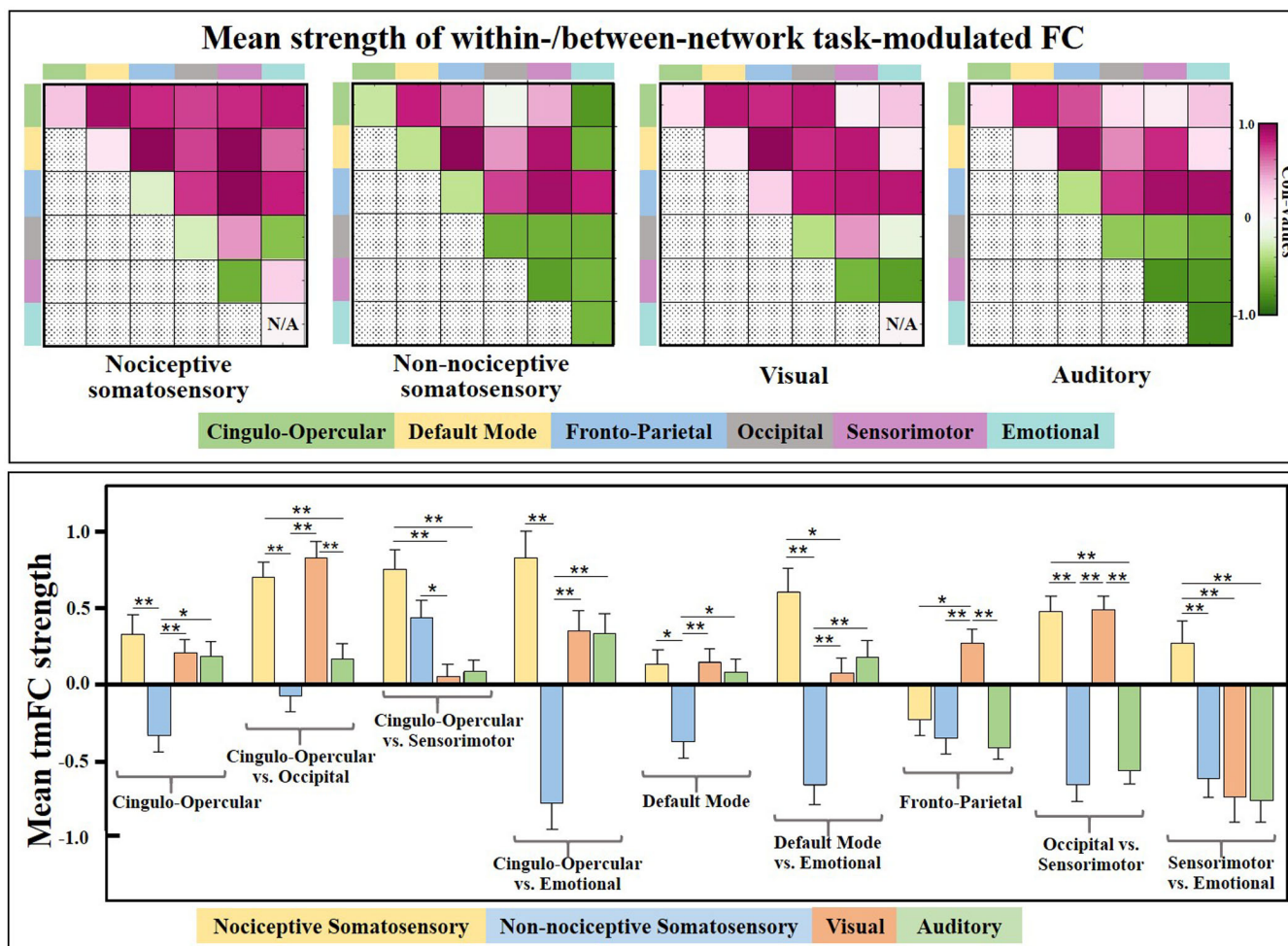


FIGURE 4 Top panel: averaged task-modulated functional connectivity (FC) strength (psychophysiological interaction [PPI] effects) for each sensory modality (diagonal = within-network, off-diagonal = between-network), and FC strength was calculated as the contrasts of interest using the constructed general linear model (GLM) models for PPI analysis; no region of interest (ROI) pairs within the emotional network was obtained for significant group effect during nociceptive somatosensory and visual stimulation (marked as “N/A”). The strength of task-modulated FC was indicated in the color bar. Bottom panel: within- and between-network comparisons with significant differences among four sensory modalities were shown; for each comparison, four colorful bars represent the mean task-modulated FC strength of each sensory modality (error bars represent the SD); *p*-values were obtained from one-way repeated-measure ANOVA analysis and Bonferroni post hoc paired comparisons (* *p* < .05, ***p* < .005)

patterns is not sufficient to characterize the responses of the complex and interconnected brain (Bullmore & Sporns, 2012; Cole et al., 2013). Pain studies using high-temporal-resolution imaging techniques, such as electroencephalography and magnetoencephalography, have shown that somatosensory stimulation could elicit rapid changes of FC among elicited neural sources (Hu, Zhang, & Hu, 2012). Therefore, segregated brain regions without information transmission are insufficient to produce the perception of pain, and only considering local activations ignore the important functional communication between regions during pain perception.

In the field of pain research, two FC analysis approaches have been applied to task-based fMRI studies: DCM and PPI. Song et al. (2021) used DCM approach to investigate the hierarchical organization for the processing of nociceptive and tactile information in the somatosensory system. For DCM analysis, pre-defined ROIs and clear hypotheses are needed. Specifically, researchers need to define

multiple and competing statistical models based on different assumptions regarding how predefined ROIs interact and how experimental manipulations modulate those interactions (Friston, Harrison, & Penny, 2003). Therefore, DCM cannot be used to check whole-brain FC changes during the task. Also, the selection of DCM models and ROIs has a huge effect on the results. For example, two multisensory comparison studies of pain applied DCM to test whether nociceptive and non-nociceptive information is processed in the primary and secondary somatosensory cortices in parallel, and they achieved largely different results (Khoshnejad, Piché, Saleh, Duncan, & Rainville, 2014; Liang, Mouraux, & Iannetti, 2011). PPI can also be used to estimate FC changes during a task and ROI-based PPI analysis has been adopted in previous neuroimaging works to examine task-modulated FC in pain (Ploner et al., 2011; Reicherts et al., 2017). For example, consistent with our results, a stronger task-modulated FC effect was observed between the amygdala of the emotional network and the

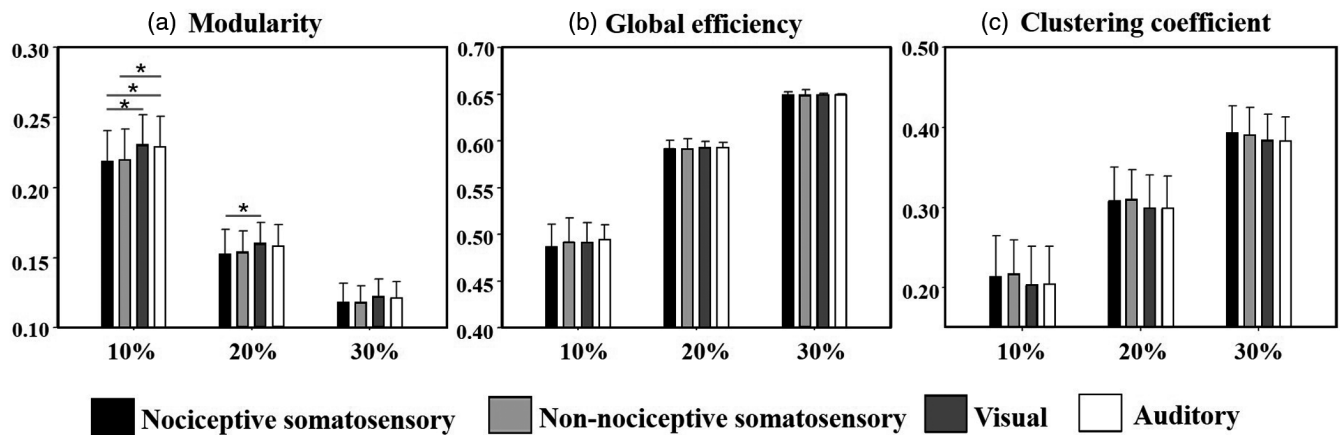


FIGURE 5 Comparison of three network properties (modularity, global efficiency, and clustering coefficient) of task-modulated functional connectivity (FC) among four different sensory modalities. The absolute psychophysiological interaction (PPI) effect matrix was thresholded at three sparsity levels (10, 20, and 30%), and the network properties were calculated separately. * $p < .05$ for Bonferroni corrected post hoc tests. The error bars represent the SD of each group

TABLE 1 The confusion matrix showing the results of cross-sensory modality prediction using psychophysiological interaction (PPI) matrices

		Predicted class							
		Nociceptive somatosensory		Non-nociceptive somatosensory		Visual		Auditory	
		Successful rate	<i>p</i> -value	Successful rate	<i>p</i> -value	Successful rate	<i>p</i> -value	Successful rate	<i>p</i> -value
Actual class	Nociceptive somatosensory	44%	<.001**	20%	.824	18%	.921	19%	.873
	Non-nociceptive somatosensory	28%	.253	25%	.428	23%	.677	25%	.431
	Visual	21%	.761	23%	.642	38%	.003**	19%	.876
	Auditory	14%	.988	33%	.049*	14%	.989	40%	.001**

Note: The statistical significance *p*-value was calculated based on 1,000 permutations (* $p < .05$, ** $p < 0.005$).

anterior insula of the cingulo-opercular network during acute pain perception (Reicherts et al., 2017). The ROI-based PPI analysis is usually done by choosing activation regions of the selected contrast of interest because it assumes that only activated or deactivated brain regions have changed FC. However, consistent with previous studies, we found that there was no clear relationship between regional activations (activated/deactivated/nonactivated) and FC changes (increased/decreased; Di & Biswal, 2019). Therefore, the whole-brain PPI, as conducted in the current study, could expand the coverage of brain regions under investigation, thus enabling the identification of more task-related regions and connections during stimulation of nociceptive pain and other sensory modalities.

4.2 | Task-modulated FC preferentially elicited by nociceptive pain

Task fMRI experiments and whole-brain PPI analysis allow us to investigate FC changes, within and between different brain networks,

related to pain processing. During the resting state, there is stronger/positive within-network FC and weaker/negative between-network FC (Bullmore & Sporns, 2012; Chai, Castañón, Ongür, & Whitfield-Gabrieli, 2012; Greicius, Krasnow, Reiss, & Menon, 2003). According to the whole-brain PPI analysis results, external sensory stimulation alters the baseline network FC and produces a task-specific FC pattern (Petersen & Sporns, 2015), that is, increases of between-network FC and decrease of within-network FC. Decreased within-network FC and increased between-network FC may reflect a rebalance to ensure efficient communication at the whole-brain level (Di & Biswal, 2019). More specifically, compared with non-nociceptive somatosensory, nociceptive somatosensory stimulation elicited more wide-spread and stronger FC within the cingulo-opercular network, between the default mode and emotional networks, and between the cingulo-opercular and emotional networks; compared with visual and auditory stimulation, nociceptive somatosensory stimulation elicited stronger FC between the cingulo-opercular and sensorimotor networks.

The default mode network is perhaps the most studied large-scale brain network and its definition was based on the observation of

consistently decreased activities during goal-oriented tasks (Andrews-Hanna, Reidler, Sepulcre, Poulin, & Buckner, 2010; Raichle et al., 2001). Default mode network generally has negative FC with other task-positive networks during resting-state, but it had widespread positive between-network task-modulated FC during stimulation of all four sensory modalities. This supports the task-general role of the default mode network as proposed in (Utevsky, Smith, & Huettel, 2014). But, task-positive networks may have different interactions with the default mode network during the perception of different sensory modalities. For example, compared with the baseline, information integration between the default mode network and emotional network increased during the nociceptive somatosensory stimulation but decreased during non-nociceptive somatosensory stimulation. The default mode network is involved in general monitoring of the environment and the fulfillment of its function should be accompanied by increased FC with regions of other brain networks (Elton & Gao, 2015). Hence, for nociceptive somatosensory, the task-modulated FC between the default mode network and the emotional network may be related to the affective dimension of nociceptive pain processing (Neugebauer, Li, Bird, & Han, 2004; Phelps & LeDoux, 2005). For non-nociceptive somatosensory stimulation, the task-modulated FC between the default mode network and the emotional network was negative. The decreased task-modulated FC may suggest less interference from task-unrelated regions to ensure more efficient communications among task-related regions (Di & Biswal, 2019). Therefore, the non-nociceptive somatosensory showed positive task-modulated FC for the sensorimotor network and negative task-modulated FC for the emotional network, since the sensory component is more prominent for non-nociceptive somatosensory information processing.

The cingulo-opercular network, centered on the anterior insula and the anterior cingulate cortex, is usually referred to as a “salience” network and closely related to pain perception (Borsook et al., 2013; Seeley et al., 2007). As one of the most consistently observed task-positive networks, the cingulo-opercular network is generally believed to undertake the fundamental function of tonic alertness by integrating sensory information to assess the homeostatic relevance or “salience” of internal and external stimuli (Sadaghiani & D'Esposito, 2015). The salience network serves as a “switch” between the default-mode network and other task-positive networks, because it evaluates extrinsic stimuli as worthy or unworthy of further attentional resources (Menon, 2015; Sridharan, Levitin, & Menon, 2008; Zhou et al., 2018). In the present study, stronger task-modulated FC between the cingulo-opercular and sensorimotor networks was observed during somatosensory stimulation. This is an intuitive finding because it is well established that both nociceptive and non-nociceptive somatosensory inputs are processed in the somatosensory cortex (Mountcastle, 2005). Similarly, visual stimulation-induced stronger task-modulated FC between the cingulo-opercular and occipital networks. Furthermore, both visual and nociceptive somatosensory stimulation-induced significantly increased task-modulated FC between the occipital, cingulo-opercular, and sensorimotor networks. This can be explained by the multisensory visual-motor integration and the involvement of the occipital areas in pain processing through descending inhibitory

mechanism (Reis et al., 2010). It is worth noting that, as compared with the other three sensory modalities, nociceptive somatosensory stimulation elicited enhanced task-modulated FC between the cingulo-opercular, sensorimotor, and emotional networks. This may be explained by the inherently highly salient content of nociceptive input, which is related to both the sensory-discriminative and affective-motivational dimensions of the complex experience of pain (Apkarian et al., 2005).

Similar to the cingulo-opercular network, the fronto-parietal network is another consistently observed brain network that involves task-positive regions (Dosenbach et al., 2007; Seeley et al., 2007). The fronto-parietal network is a control-type network and it is involved in a wide variety of tasks by initiating and modulating cognitive control abilities (Dosenbach, Fair, Cohen, Schlaggar, & Petersen, 2008). For all four sensory modalities, significant positive task-modulated FC was observed between the cingulo-opercular and fronto-parietal networks. This supports the recognized role of these frontal and parietal areas in attention: they are involved in selectively biasing the cortical processing of incoming sensory inputs according to their salience and relevance (Corbetta & Shulman, 2002; Yantis, 2008).

By comparing graph-theory network configurations of the task-induced coactivation networks and resting-state networks, a previous study found that the brain during task exhibits smaller modularity and greater small-worldness that facilitate both regional and global information transmission (Xin, Suril, Kim, & Biswal, 2013). Small modularity has been observed during noxious somatosensory stimulation compared with innocuous somatosensory stimulation in a research study, suggesting pain integrates brain systems into fewer functional communities (Zheng et al., 2020). Here we made a further comparison of global network properties for task-modulated FC networks among different sensory modalities. FC networks modulated by nociceptive/non-nociceptive somatosensory stimulation showed smaller modularity compared with visual and auditory, and this could be related to the more high-level cognitive activities involved during the perception of somatosensory stimulation (Gonzalez-Castillo & Bandettini, 2018; Kitzbichler, Henson, Smith, Nathan, & Bullmore, 2011; Vatansever, Menon, Manktelow, Sahakian, & Stamatakis, 2015). At present, the use of graphic network metrics in task-modulated FC network research is still in its infancy, and our results here provide more evidence that graphic network analysis is valuable for capturing cognitive processes during task conditions.

This work also used the task-modulated FC patterns (whole-brain PPI matrices) to predict the sensory modality that the participants perceived, with the aim to validate the reliability of PPI features. Because fMRI measures suffer from low reliability in general (Elliott et al., 2020), PPI, as a higher-order measure than conventional task activations and FC, may also have low reliability. Indeed, a study has demonstrated very limited reliability of PPI effects in a simple visual task (Di & Biswal, 2017). To show the PPI patterns elicited by different sensory modalities were accurate, reliable, and closely related to corresponding sensory modalities, we performed cross-modality prediction analysis using the whole-brain PPI effects as features. We found better-than-chance classification accuracies, especially for the nociceptive somatosensory stimulation, supporting the potential use of multivariate statistics to reflect behavioral phenotypes.

4.3 | Limitations and future work

Several limitations of this study should be mentioned here. First, the task-modulated FC patterns were inferred from PPI effects, which can only estimate unidirectional relationships among brain regions and is unable to reveal directional (causal) information flow among multiple brain regions. As mentioned earlier, DCM can characterize causal relationships, but it can hardly be used for the whole brain. Multivariate Granger causality analysis may be a potential tool to infer the directional relationship among brain regions in a task, but it also suffers from the high dimensionality and a limited number of samples of fMRI. New and efficient whole-brain directional FC estimation methods will advance our knowledge about task-modulated FC during nociceptive perception. Second, the cerebellar network was not included in the whole-brain PPI analysis here because of the incomplete coverage of the cerebellum of several subjects. Third, because the resting-state FC and task-modulated FC were calculated by two different methods, it is inappropriate to directly compare these two types of FC in terms of FC strength or graphic metrics. Fourth, mathematically, the PPI approach is based on a regression model, and the task-modulated FC matrix is not symmetric, depending on whether one region is used as a seed (independent variable) or a dependent variable. Indeed, if FC between two regions is modulated by a task (no matter in which direction or in both directions), a PPI effect is likely significant no matter which region is used as seed or dependent variable. Therefore, it is a common practice in current literature to symmetrize a PPI matrix without considering the difference between lower and upper diagonal elements. There is indeed a certain degree of difference in the PPI effects between the two directions (see Figures S2 and S3), and the symmetrization procedure might cause the loss of some useful information about the network structure of task-modulated FC. Therefore, analysis of the PPI effects without symmetrizing might obtain different results. However, in order to keep consistency with literature for a fair comparison and to ensure the interpretability of the results, the PPI matrices were symmetrized by averaging corresponding lower and upper diagonal elements. Last but not least, the findings of this study are potentially useful in the development of a new and objective tool of pain assessment in clinical practices because these task-modulated FC patterns can effectively distinguish the perception of pain from other types of sensory perception. However, the current results were obtained with healthy subjects and transient stimuli of nociceptive pain and other sensory modalities, which limit the translational applications of this study. Future studies are needed to investigate task-modulated FC related to pain perception in patients with chronic pain.

5 | CONCLUSION

We performed a multisensory comparative study of whole-brain task-modulated FC in healthy subjects, with the aim to reveal whether nociceptive pain could elicit different task-modulated FC patterns from other sensory modalities. We identified broader involvement of

brain networks for all four sensory modalities and found differences in regional and global features of task-modulated FC networks for nociceptive somatosensory, as compared with the other three sensory modalities. Specifically, nociceptive somatosensory stimulation elicits more widespread and stronger within-/between-network task-modulated FC of the default mode, the cingulo-opercular, and the fronto-parietal networks, and the task-modulated FC network elicited by nociceptive stimulation also has smaller modularity. The results obtained in the present study could provide new insights from the perspective of task-modulated FC networks into the neural mechanisms of pain processing.

ACKNOWLEDGMENTS

We gratefully acknowledge all the participants. This research was supported by the National Natural Science Foundation of China (No. 81901831 and 81871443), the Natural Science Foundation of Guangdong Province, China (No. 2021A1515011152), and Shenzhen-Hong Kong Institute of Brain Science-Shenzhen Fundamental Research Institutions (No. 2021SHIBS0003).

CONFLICT OF INTEREST

The authors declare no potential conflict of interest.

AUTHOR CONTRIBUTIONS

Zhiguo Zhang: Designed, provided funding and supervised data analysis; **Li Zhang, Zhen Liang, and Gan Huang:** Supervised data collection and contributed to revising the article for technical and intellectual content; **Huijuan Zhang:** Recruited participants and collected data; **Xin Di:** Verified the analytical methods; **Linling Li:** Conducted all data analysis and wrote the article; all authors reviewed the findings and interpretation.

DATA AVAILABILITY STATEMENT

Raw data of this study are available from the corresponding authors upon reasonable request.

ETHICS STATEMENT

This study was approved by the ethics committee of the Institute of Psychology, Chinese Academy of Sciences (date of approval: November 2016; approval number: H16021). All subjects gave their written informed consent.

ORCID

Linling Li  <https://orcid.org/0000-0001-7767-7202>

Li Zhang  <https://orcid.org/0000-0003-1641-7831>

REFERENCES

- Achard, S., & Bullmore, E. (2007). Efficiency and cost of economical brain functional networks. *PLoS Computational Biology*, 3(2), e17. <https://doi.org/10.1371/journal.pcbi.0030017>
- Andrews-Hanna, J. R., Reidler, J. S., Sepulcre, J., Poulin, R., & Buckner, R. L. (2010). Functional-anatomic fractionation of the brain's default network. *Neuron*, 65(4), 550–562. <https://doi.org/10.1016/j.neuron.2010.02.005>

- Apkarian, A. V., Bushnell, M. C., Treede, R. D., & Zubieta, J. K. (2005). Human brain mechanisms of pain perception and regulation in health and disease. *European Journal of Pain*, 9(4), 463–484. <https://doi.org/10.1016/j.ejpain.2004.11.001>
- Benjamini, Y., & Hochberg, Y. (1995). Controlling the false discovery rate: A practical and powerful approach to multiple testing. *Journal of Royal Statistical Society. Series B (Methodological)*, 57(1), 289–300. <https://doi.org/10.1111/j.2517-6161.1995.tb02031.x>
- Benjamini, Y., & Yekutieli, D. (2001). The control of the false discovery rate in multiple testing under dependency. *The Annals of Statistics*, 29(4), 1165–1188.
- Borsook, D., Edwards, R., Elman, I., Becerra, L., & Levine, J. (2013). Pain and analgesia: The value of salience circuits. *Progress in Neurobiology*, 104, 93–105. <https://doi.org/10.1016/j.pneurobio.2013.02.003>
- Bullmore, E., & Sporns, O. (2009). Complex brain networks: Graph theoretical analysis of structural and functional systems. *Nature Review Neuroscience*, 10(3), 186–198. <https://doi.org/10.1038/nrn2575>
- Bullmore, E., & Sporns, O. (2012). The economy of brain network organization. *Nature Review Neuroscience*, 13, 336–349. <https://doi.org/10.1038/nrn3214>
- Bullmore, E. T., & Bassett, D. S. (2011). Brain graphs: Graphical models of the human brain connectome. *Annual Review of Clinical Psychology*, 7(7), 113–140. <https://doi.org/10.1146/annurev-clinpsy-040510-143934>
- Chai, X. J., Castañón, A. N., Ongür, D., & Whitfield-Gabrieli, S. (2012). Anticorrelations in resting state networks without global signal regression. *NeuroImage*, 59(2), 1420–1428. <https://doi.org/10.1016/j.neuroimage.2011.08.048>
- Cohen, J. R., & D'Esposito, M. (2016). The segregation and integration of distinct brain networks and their relationship to cognition. *Journal of Neuroscience*, 36(48), 12083–12094. <https://doi.org/10.1523/jneurosci.2965-15.2016>
- Cole, M. W., Ito, T., Schultz, D., Mill, R., Chen, R., & Cocuzza, C. (2019). Task activations produce spurious but systematic inflation of task functional connectivity estimates. *NeuroImage*, 189, 1–18. <https://doi.org/10.1016/j.neuroimage.2018.12.054>
- Cole, M. W., Reynolds, J. R., Power, J. D., Repovs, G., Anticevic, A., & Braver, T. S. (2013). Multi-task connectivity reveals flexible hubs for adaptive task control. *Nature Neuroscience*, 16(9), 1348–1355. <https://doi.org/10.1038/nn.3470>
- Corbetta, M., & Shulman, G. L. (2002). Control of goal-directed and stimulus-driven attention in the brain. *Nature Review Neuroscience*, 3(3), 201–215. <https://doi.org/10.1038/nrn755>
- Craddock, R. C., Jbabdi, S., Yan, C.-G., Vogelstein, J. T., Castellanos, F. X., Di Martino, A., ... Milham, M. P. (2013). Imaging human connectomes at the macroscale. *Nature Methods*, 10(6), 524–539. <https://doi.org/10.1038/nmeth.2482>
- Di, X., & Biswal, B. B. (2017). Psychophysiological interactions in a visual checkerboard task: Reproducibility, reliability, and the effects of deconvolution. *Frontiers in Neuroscience*, 11, 573. <https://doi.org/10.3389/fnins.2017.00573>
- Di, X., & Biswal, B. B. (2019). Toward task connectomics: Examining whole-brain task modulated connectivity in different task domains. *Cerebral Cortex*, 29(4), 1572–1583. <https://doi.org/10.1093/cercor/bhy055>
- Di, X., Gohel, S., Kim, E. H., & Biswal, B. B. (2013). Task vs. rest-different network configurations between the coactivation and the resting-state brain networks. *Frontiers in Human Neuroscience*, 7, 493–493. <https://doi.org/10.3389/fnhum.2013.00493>
- Di, X., Reynolds, R. C., & Biswal, B. B. (2017). Imperfect (de)convolution may introduce spurious psychophysiological interactions and how to avoid it. *Human Brain Mapping*, 38(4), 1723–1740. <https://doi.org/10.1002/hbm.23413>
- Di, X., Zhang, Z., & Biswal, B. B. (2020). Understanding psychophysiological interaction and its relations to beta series correlation. *Brain Imaging and Behavior*, 322073, 958–973. <https://doi.org/10.1007/s11682-020-00304-8>
- Dosenbach, N. U., Fair, D. A., Cohen, A. L., Schlaggar, B. L., & Petersen, S. E. (2008). A dual-networks architecture of top-down control. *Trends in Cognitive Science*, 12(3), 99–105. <https://doi.org/10.1016/j.tics.2008.01.001>
- Dosenbach, N. U., Fair, D. A., Miezin, F. M., Cohen, A. L., Wenger, K. K., Dosenbach, R. A., ... Petersen, S. E. (2007). Distinct brain networks for adaptive and stable task control in humans. *Proceedings of the National Academy of Sciences of the United States of America*, 104(26), 11073–11078. <https://doi.org/10.1073/pnas.0704320104>
- Dosenbach, N. U., Nardos, B., Cohen, A. L., Fair, D. A., Power, J. D., Church, J. A., ... Schlaggar, B. L. (2010). Prediction of individual brain maturity using fMRI. *Science*, 329(5997), 1358–1361. <https://doi.org/10.1126/science.1194144>
- Downar, J., Crawley, A. P., Mikulis, D. J., & Davis, K. D. (2000). A multi-modal cortical network for the detection of changes in the sensory environment. *Nature Neuroscience*, 3(3), 277–283. <https://doi.org/10.1038/72991>
- Duerden, E. G., & Albanese, M. C. (2013). Localization of pain-related brain activation: A meta-analysis of neuroimaging data. *Human Brain Mapping*, 34(1), 109–149. <https://doi.org/10.1002/hbm.21416>
- Elliott, M. L., Knodt, A. R., Ireland, D., Morris, M. L., Poulton, R., Ramrakha, S., ... Hariri, A. R. (2020). What is the test-retest reliability of common task-functional MRI measures? New empirical evidence and a meta-analysis. *Psychological Science*, 31(7), 792–806. <https://doi.org/10.1177/0956797620916786>
- Elton, A., & Gao, W. (2015). Task-positive functional connectivity of the default mode network transcends task domain. *Journal of Cognitive Neuroscience*, 27(12), 2369–2381. https://doi.org/10.1162/jocn_a_00859
- Friston, K. J., Buechel, C., Fink, G. R., Morris, J., Rolls, E., & Dolan, R. J. (1997). Psychophysiological and modulatory interactions in neuroimaging. *NeuroImage*, 6(3), 218–229. <https://doi.org/10.1006/nimg.1997.0291>
- Friston, K. J., Harrison, L., & Penny, W. (2003). Dynamic causal modelling. *NeuroImage*, 19(4), 1273–1302. [https://doi.org/10.1016/S1053-8119\(03\)00202-7](https://doi.org/10.1016/S1053-8119(03)00202-7)
- Gonzalez-Castillo, J., & Bandettini, P. A. (2018). Task-based dynamic functional connectivity: Recent findings and open questions. *NeuroImage*, 180 (Pt B), 526–533. <https://doi.org/10.1016/j.neuroimage.2017.08.006>
- Greicius, M. D., Krasnow, B., Reiss, A. L., & Menon, V. (2003). Functional connectivity in the resting brain: A network analysis of the default mode hypothesis. *Proceedings of the National Academy of Sciences of the United States of America*, 100(1), 253–258. <https://doi.org/10.1073/pnas.0135058100>
- Hu, L., Zhang, Z. G., & Hu, Y. (2012). A time-varying source connectivity approach to reveal human somatosensory information processing. *NeuroImage*, 62(1), 217–228. <https://doi.org/10.1016/j.neuroimage.2012.03.094>
- Iannetti, G. D., & Mouraux, A. (2010). From the neuromatrix to the pain matrix (and back). *Experimental Brain Research*, 205(1), 1–12. <https://doi.org/10.1007/s00221-010-2340-1>
- Ibinson, J. W., Vogt, K. M., Taylor, K. B., Dua, S. B., Becker, C. J., Loggia, M., & Wasan, A. D. (2015). Optimizing and interpreting insular functional connectivity maps obtained during acute experimental pain: The effects of global signal and task paradigm regression. *Brain Connectivity*, 5(10), 649–657. <https://doi.org/10.1089/brain.2015.0354>
- Khoshnejad, M., Piché, M., Saleh, S., Duncan, G., & Rainville, P. (2014). Serial processing in primary and secondary somatosensory cortex: A DCM analysis of human fMRI data in response to innocuous and noxious electrical stimulation. *Neuroscience Letters*, 577, 83–88. <https://doi.org/10.1016/j.neulet.2014.06.013>

- Kitzbichler, M. G., Henson, R. N., Smith, M. L., Nathan, P. J., & Bullmore, E. T. (2011). Cognitive effort drives workspace configuration of human brain functional networks. *Journal of Neuroscience*, 31(22), 8259–8270. <https://doi.org/10.1523/jneurosci.0440-11.2011>
- Kong, J., Loggia, M. L., Zyloney, C., Tu, P., Laviolette, P., & Gollub, R. L. (2010). Exploring the brain in pain: Activations, deactivations and their relation. *Pain*, 148(2), 257–267. <https://doi.org/10.1016/j.pain.2009.11.008>
- Kucyi, A., & Davis, K. D. (2015). The dynamic pain connectome. *Trends in Cognitive Science*, 38(2), 86–95. <https://doi.org/10.1016/j.tins.2014.11.006>
- Legrain, V., Iannetti, G. D., Plaghki, L., & Mouraux, A. (2011). The pain matrix reloaded: A salience detection system for the body. *Progress in Neurobiology*, 93(1), 111–124. <https://doi.org/10.1016/j.pneurobio.2010.10.005>
- Liang, M., Mouraux, A., Hu, L., & Iannetti, G. D. (2013). Primary sensory cortices contain distinguishable spatial patterns of activity for each sense. *Nature Communications*, 4, 1979. <https://doi.org/10.1038/ncomms2979>
- Liang, M., Mouraux, A., & Iannetti, G. D. (2011). Parallel processing of nociceptive and non-nociceptive somatosensory information in the human primary and secondary somatosensory cortices: Evidence from dynamic causal modeling of functional magnetic resonance imaging data. *Journal of Neuroscience*, 31(24), 8976–8985. <https://doi.org/10.1523/jneurosci.6207-10.2011>
- Liang, M., Su, Q., Mouraux, A., & Iannetti, G. D. (2019). Spatial patterns of brain activity preferentially reflecting transient pain and stimulus intensity. *Cerebral Cortex*, 29(5), 2211–2227. <https://doi.org/10.1093/cercor/bhz026>
- McLaren, D. G., Ries, M. L., Xu, G., & Johnson, S. C. (2012). A generalized form of context-dependent psychophysiological interactions (gPPI): A comparison to standard approaches. *NeuroImage*, 61(4), 1277–1286. <https://doi.org/10.1016/j.neuroimage.2012.03.068>
- Menon, V. (2015). Salience network. In A. W. Toga (Ed.), *Brain mapping: An encyclopedic reference* (Vol. 2, pp. 597–611). St. Louis, MO: Elsevier.
- Mountcastle, V. B. (2005). *The sensory hand: Neural mechanisms of somatic sensation*. Cambridge, MA: Harvard University Press.
- Mouraux, A., Diukova, A., Lee, M. C., Wise, R. G., & Iannetti, G. D. (2011). A multisensory investigation of the functional significance of the “pain matrix”. *NeuroImage*, 54(3), 2237–2249. <https://doi.org/10.1016/j.neuroimage.2010.09.084>
- Necka, E. A., Lee, I.-S., Kucyi, A., Cheng, J. C., Yu, Q., & Atlas, L. Y. (2019). Applications of dynamic functional connectivity to pain and its modulation. *Pain Reports*, 4(4), e752. <https://doi.org/10.1097/PR9.0000000000000752>
- Neugebauer, V., Li, W., Bird, G. C., & Han, J. S. (2004). The amygdala and persistent pain. *The Neuroscientist*, 10(3), 221–234. <https://doi.org/10.1177/1073858403261077>
- Newman, M. E. J. (2006). Modularity and community structure in networks. *Proceedings of the National Academy of Sciences of the United States of America*, 103(23), 8577–8582. <https://doi.org/10.1073/pnas.0601602103>
- O'Reilly, J. X., Woolrich, M. W., Behrens, T. E. J., Smith, S. M., & Johansen-Berg, H. (2012). Tools of the trade: Psychophysiological interactions and functional connectivity. *Social Cognitive & Affective Neuroscience*, 7(5), 604–609. <https://doi.org/10.1093/scan/nns055>
- Petersen, S. E., & Sporns, O. (2015). Brain networks and cognitive architectures. *Neuron*, 88(1), 207–219. <https://doi.org/10.1016/j.neuron.2015.09.027>
- Phelps, E. A., & LeDoux, J. E. (2005). Contributions of the amygdala to emotion processing: From animal models to human behavior. *Neuron*, 48(2), 175–187. <https://doi.org/10.1016/j.neuron.2005.09.025>
- Ploner, M., Lee, M. C., Wiech, K., Bingel, U., & Tracey, I. (2011). Flexible cerebral connectivity patterns subserve contextual modulations of pain. *Cerebral Cortex*, 21(3), 719–726. <https://doi.org/10.1093/cercor/bhq146>
- Raichle, M. E., MacLeod, A. M., Snyder, A. Z., Powers, W. J., Gusnard, D. A., & Shulman, G. L. (2001). A default mode of brain function. *Proceedings of the National Academy of Sciences of the United States of America*, 98(2), 676–682. <https://doi.org/10.1073/pnas.98.2.676>
- Reicherts, P., Wiemer, J., Gerdes, A. B. M., Schulz, S. M., Pauli, P., & Wieser, M. J. (2017). Anxious anticipation and pain: The influence of instructed vs conditioned threat on pain. *Social Cognitive & Affective Neuroscience*, 12(4), 544–554. <https://doi.org/10.1093/scan/nsw181>
- Reis, G. M., Dias, Q. M., Silveira, J. W., Del Vecchio, F., Garcia-Cairasco, N., & Prado, W. A. (2010). Antinociceptive effect of stimulating the occipital or retrosplenial cortex in rats. *Journal of Pain*, 11(10), 1015–1026. <https://doi.org/10.1016/j.jpain.2010.01.269>
- Rubinov, M., & Sporns, O. (2010). Complex network measures of brain connectivity: Uses and interpretations. *NeuroImage*, 52(3), 1059–1069. <https://doi.org/10.1016/j.neuroimage.2009.10.003>
- Sabatinelli, D., Fortune, E. E., Li, Q., Siddiqui, A., Krafft, C., Oliver, W. T., ... Jeffries, J. (2011). Emotional perception: Meta-analyses of face and natural scene processing. *NeuroImage*, 54(3), 2524–2533. <https://doi.org/10.1016/j.neuroimage.2010.10.011>
- Sadaghiani, S., & D'Esposito, M. (2015). Functional characterization of the cingulo-occipular network in the maintenance of tonic alertness. *Cerebral Cortex*, 25(9), 2763–2773. <https://doi.org/10.1093/cercor/bhu072>
- Seeley, W. W., Menon, V., Schatzberg, A. F., Keller, J., Glover, G. H., Kenna, H., ... Greicius, M. D. (2007). Dissociable intrinsic connectivity networks for salience processing and executive control. *Journal of Neuroscience*, 27(9), 2349–2356. <https://doi.org/10.1523/jneurosci.5587-06.2007>
- Song, Y., Su, Q., Yang, Q., Zhao, R., Yin, G., Qin, W., ... Liang, M. (2021). Feedforward and feedback pathways of nociceptive and tactile processing in human somatosensory system: A study of dynamic causal modeling of fMRI data. *NeuroImage*, 234, 117957. <https://doi.org/10.1016/j.neuroimage.2021.117957>
- Sridharan, D., Levitin, D. J., & Menon, V. (2008). A critical role for the right fronto-insular cortex in switching between central-executive and default-mode networks. *Proceedings of the National Academy of Sciences of the United States of America*, 105(34), 12569–12574. <https://doi.org/10.1073/pnas.0800005105>
- Su, Q., Qin, W., Yang, Q. Q., Yu, C. S., Qian, T. Y., Mouraux, A., ... Liang, M. (2019). Brain regions preferentially responding to transient and iso-intense painful or tactile stimuli. *NeuroImage*, 192, 52–65. <https://doi.org/10.1016/j.neuroimage.2019.01.039>
- Utevsky, A. V., Smith, D. V., & Huettel, S. A. (2014). Precuneus is a functional core of the default-mode network. *Journal of Neuroscience*, 34(3), 932–940. <https://doi.org/10.1523/jneurosci.4227-13.2014>
- Vatansver, D., Menon, D. K., Manktelow, A. E., Sahakian, B. J., & Stamatakis, E. A. (2015). Default mode dynamics for global functional integration. *Journal of Neuroscience*, 35(46), 15254–15262. <https://doi.org/10.1523/jneurosci.2135-15.2015>
- Vogt, K. M., Becker, C. J., Wasan, A. D., & Ibinson, J. W. (2016). Human posterior insula functional connectivity differs between electrical pain and the resting state. *Brain Connectivity*, 6(10), 786–794. <https://doi.org/10.1089/brain.2016.0436>
- Watts, D. J., & Strogatz, S. H. (1998). Collective dynamics of 'small-world' networks. *Nature*, 393(6684), 440–442. <https://doi.org/10.1038/30918>
- Xin, D., Suril, G., Kim, E. H., & Biswal, B. B. (2013). Task vs. rest—Different network configurations between the coactivation and the resting-state brain networks. *Frontiers in Human Neuroscience*, 7, 493.
- Yantis, S. (2008). The neural basis of selective attention: Cortical sources and targets of attentional modulation. *Current Directions in*

Psychological Science, 17(2), 86–90. <https://doi.org/10.1111/j.1467-8721.2008.00554.x>

Yao, Z., Hu, B., Xie, Y., Moore, P., & Zheng, J. (2015). A review of structural and functional brain networks: Small world and atlas. *Brain Informatics*, 2(1), 45–52. <https://doi.org/10.1007/s40708-015-0009-z>

Zheng, W., Woo, C.-W., Yao, Z., Goldstein, P., Atlas, L. Y., Roy, M., ... Wager, T. D. (2020). Pain-evoked reorganization in functional brain networks. *Cerebral Cortex*, 30(5), 2804–2822. <https://doi.org/10.1093/cercor/bhz276>

Zhou, Y., Friston, K. J., Zeidman, P., Chen, J., Li, S., & Razi, A. (2018). The hierarchical organization of the default, dorsal attention and salience networks in adolescents and young adults. *Cerebral Cortex*, 28(2), 726–737. <https://doi.org/10.1093/cercor/bhx307>

SUPPORTING INFORMATION

Additional supporting information may be found in the online version of the article at the publisher's website.

How to cite this article: Li, L., Di, X., Zhang, H., Huang, G., Zhang, L., Liang, Z., & Zhang, Z. (2022). Characterization of whole-brain task-modulated functional connectivity in response to nociceptive pain: A multisensory comparison study. *Human Brain Mapping*, 43(3), 1061–1075. <https://doi.org/10.1002/hbm.25707>